AIAA 2002–0714

An Implicit-Explicit Hybrid Scheme for Calculating Complex Unsteady Flows

John M. Hsu
Antony Jameson
Department of Aeronautics and Astronautics
Stanford University
Stanford, California 94305 U.S.A.

40th AIAA Aerospace Sciences Meeting and Exhibit
January 14–17, 2002/Reno, Nevada

An Implicit-Explicit Hybrid Scheme for Calculating Complex Unsteady Flows

John M. Hsu*
Antony Jameson†
Department of Aeronautics and Astronautics
Stanford University
Stanford, California 94305 U.S.A.

In current practice, unsteady flow simulations for turbomachinery are performed using a dual-time-stepping scheme. This work is motivated by the need to solve the time-accurate Navier-Stokes equations with greatly decreased computational cost. The purpose of this paper is to investigate the introduction of an initial ADI step, guaranteeing second order accuracy in time, followed by a small number of cycles of the dual-time-stepping scheme augmented by multigrid. The $O\left(\Delta t^2\right)$ accuracy in time should be retained without the need for large numbers of inner iterations required for convergence of typical iterative methods. The details of this new scheme are presented in this paper while examples are given to demonstrate the second order accuracy and the convergence properties of the scheme.

Introduction

Current calculations of complex unsteady flows are prohibitively expensive for use in real engineering applications to turbomachinery design. Typical flow solvers for unsteady integration employ a fully implicit time stepping scheme, in which the equations are solved by an inner iteration. In the ASCI Turbomachinery code TFLO which is under development at Stanford, an explicit multigrid scheme is used for the inner iterations which advances to a steady state in fictitious time. In order to achieve convergence within each physical time step, these dual-time-stepping schemes require a substantial number of pseudo-time steps (typically between 30-100, depending on the case). In the Stanford ASCI project, we are calculating the unsteady flow through a complete turbine with 9 blade rows; using a mesh with 94 million cells. Using an implicit scheme, the number of time steps required to reach a stationary periodic state is ~ 2500, and the total estimated computer time is 2.0 million CPU hours. One disadvantage of the current implementation is that using 512 processors, the calculation requires approximately 8 months. Another disadvantage of the dual-time-stepping method is that there are no available error estimates for time accuracy available unless the inner iterations are fully converged, although numerical experiments have demonstrated second order accuracy in time.

In order to perform the full unsteady simulations of complex flows in turbomachinery feasible for engineering use, we need to improve the efficiency of the underlying numerical algorithms. Three approaches to be considered are

(1.) To search for a more rapidly convergent inner iteration method; for this purpose, a Preconditioned Symmetric Gauss-Seidel Relaxation Method is being studied,[1–3]

(2.) To reformulate the scheme so that it yields sufficient accuracy without the need for full convergence of the inner iterations, and

(3.) To consider the alternative approach of representing the solution in the frequency domain; studies of a nonlinear frequency domain approach are described by McMullen et al.[4]

In this paper, we follow the second approach. Our idea is to formulate a hybrid scheme which introduces an initial linearized alternating direction implicit (ADI) step, which ultimately provides the desired nominal second order accuracy in time. With the factorization error of the ADI Scheme restricting the time steps for which sufficient stability and accuracy can be attained, we are augmenting the ADI Scheme with a number of iterations of the dual-time-stepping scheme to reduce the errors due to both linearization and factorization; to increase the feasible time step. With the initial ADI step already providing second order accuracy, it is no longer necessary to continue the inner iterations to full convergence. Thus, the two components of the hybrid scheme complement each other to decrease computational costs.

For the case with multiple processors, the additional iterations with multigrid should provide information

*Graduate Student

†Professor. Member AIAA

exchange between processors necessary to stabilize the ADI scheme when it is run separately in each processor.

The efficiency of the hybrid scheme has been verified in this work for the simulation of the unsteady flow around a pitching airfoil, for which both alternative numerical results and experimental data are available.

Derivations

Governing Equations

The two dimensional unsteady compressible Navier-Stokes equations in the Cartesian coordinate system can be written as:

$$\frac{\partial w}{\partial t} + R(w) = 0, \quad R(w) = \frac{\partial}{\partial x_i} f_i(w) \tag{1}$$

where w is the vector of conserved flow variables

$$w = \begin{bmatrix} \rho \\ \rho u \\ \rho v \\ \rho E \end{bmatrix}$$

Given the mesh is moving with velocities u_m and v_m at each mesh point, the convective fluxes f_1 and f_2 in the corresponding x_1 and x_2 coordinate directions are

$$f_1 = f_{c_1} - f_{v_1}, \quad f_2 = f_{c_2} - f_{v_2}$$

Convective Flux are defined as

$$f_{c_1} = \begin{bmatrix} \rho u_r \\ \rho u_r u + p \\ \rho u_r v \\ \rho u_r H \end{bmatrix}, \quad f_{c_2} = \begin{bmatrix} \rho v_r \\ \rho v_r u \\ \rho v_r v + p \\ \rho v_r H \end{bmatrix}$$

where $u_r = u - u_m$ and $v_r = v - v_m$. Viscous flux are defined as

$$f_{v_1} = \begin{bmatrix} 0 \\ \tau_{xx} \\ \tau_{xy} \\ \bar{u} \cdot \bar{\tau_x} - q_x \end{bmatrix}, \quad f_{v_2} = \begin{bmatrix} 0 \\ \tau_{yx} \\ \tau_{yy} \\ \bar{u} \cdot \bar{\tau_y} - q_y \end{bmatrix}$$

where the stress tensor and its components are given by

$$\bar{\bar{\tau}} = \begin{bmatrix} \tau_{xx} & \tau_{xy} \\ \tau_{yx} & \tau_{yy} \end{bmatrix}$$

$$\begin{aligned} \tau_{xx} &= 2\mu u_x + \lambda (u_x + v_y) \\ \tau_{yy} &= 2\mu u_y + \lambda (u_x + v_y) \\ \tau_{xy} &= \tau_{yx} = \mu (u_y + v_x) \end{aligned}$$

here $\lambda = -\frac{2}{3}\mu$ and the heat flux vectors are given by

$$\begin{aligned} q_x &= -\kappa T_x \\ q_y &= -\kappa T_y \end{aligned}$$

T_x and T_y are the temperature gradients in x and y directions and the heat transfer coefficient is defined as

$$k = \gamma \left(\frac{\mu}{Pr} + \frac{\mu_{turb}}{Pr_{turb}} \right) \tag{2}$$

where μ and μ_{turb} are the laminar and turbulent kinematic viscosity, Pr and Pr_{turb} are the laminar and turbulent Prandtl's number.

For ideal gas, the equation of state may be written as

$$p = (\gamma - 1)\rho \left[E - \frac{u^2 + v^2}{2} \right]$$

Consider a control volume $\mathcal{D}$ with boundary $\mathcal{B}$, equation (1) can be rewritten in integral form

$$\frac{\partial}{\partial t} \int_{\mathcal{D}} w d\mathcal{V} + \int_{\mathcal{B}} f_i d\mathcal{S}_i = 0 \tag{3}$$

where $d\mathcal{S}_i$ is the component of area projected in the x_i direction. A set of ODE's can be obtained from the discretisation of the spatial variables when the above integral equation (3) is applied independently to each of the cells in the domain,

$$\frac{d}{dt} \left(w_{ij} \mathcal{V}_{ij} \right) + R \left(w_{ij} \right) = 0 \tag{4}$$

For a general body fitted moving coordinate system with coordinates X_1, X_2, define the determinant of the transformation as

$$J = \left| \frac{\partial \bar{x}}{\partial \bar{X}} \right|$$

the governing equations in the transformed coordinates becomes

$$\frac{\partial}{\partial t}(Jw) + \frac{\partial F_i}{\partial X_i} = 0) \tag{5}$$

where

$$F_i = J \frac{\partial X_i}{\partial x_j} f_j$$

Fully Implicit Backward Difference Formula (BDF)

Consider the implicit semidiscrete finite volume scheme (5)

$$\frac{d}{dt} \left(w_{ij}^{n+1} \mathcal{V}_{ij}^{n+1} \right) + R \left(w_{ij}^{n+1} \right) = 0 \tag{6}$$

where $R(w) = D_{X_1} F_1(w) + D_{X_2} F_2(w)$ is the discrete residual and D_{X_1} and D_{X_2} are the difference operators which approximate $\frac{\partial}{\partial X_1}$ and $\frac{\partial}{\partial X_2}$.

The Backward Difference Formulae are obtained by discretizing (6) in time using one sided schemes. For example, the second order accurate BDF is

$$\begin{aligned} \frac{3}{2\Delta t} w_{i,j}^{n+1} \mathcal{V}_{i,j}^{n+1} - \frac{4}{2\Delta t} w_{i,j}^{n} \mathcal{V}_{i,j}^{n} + \frac{1}{2\Delta t} w_{i,j}^{n-1} \mathcal{V}_{i,j}^{n-1} \\ + R \left(w_{i,j}^{n+1} \right) = 0 \end{aligned} \tag{7}$$

where $R(w_{i,j}^{n+1})$ is evaluated at the end of each time step.

This scheme is A-stable(i.e., unconditionally stable for any Δt if the physical equations are stable.). Note that the trapezoidal scheme is also A-stable and second order accurate, but it is undamped as the Δt tends toward infinity. Therefore the 3-4-1 backward difference scheme is preferred in our application.

Dual Time Stepping Scheme

The fully implicit BDF consists of coupled nonlinear equations, which have to be solved at each time step by some approximate method. One approach is the Dual Time Stepping Scheme,[5] where the nonlinear BDF is solved by inner iterations which advance in pseudo-time τ, given that the cell volume of the mesh does not change, or $\mathcal{V} = \mathcal{V}^{n+1} = \mathcal{V}^n = \mathcal{V}^{n-1}$,

$$\frac{\partial w}{\partial \tau} + \left[\frac{\mathcal{V}\left(3w^{n+1} - 4w^n + w^{n-1}\right)}{2\Delta t} + R(w) \right] = 0$$

defining the modified residual and writing the equation in delta form

$$R^*(w^n) = \left[\frac{3\mathcal{V}}{2\Delta t}\Delta w^n - \frac{\mathcal{V}}{2\Delta t}\Delta w^{n-1} + R(w^n) \right]$$

thus,

$$\frac{\partial w}{\partial \tau} + R^*(w^n) = 0 \tag{8}$$

Equation (8) is the modified steady state problem in pseudo-time. On convergence to steady state, $\frac{\partial w}{\partial \tau} = 0$, the solution of the nonlinear BDF (7) is recovered. To accelerate convergence, equation (8) is solved using

1. explicit Runge-Kutta multistage scheme with variable local $\Delta\tau$,
2. implicit residual averaging, and
3. multigrid.

The p–stage Runge–Kutta scheme is given by

$$\begin{aligned} w^{(0)} &= w^n \\ w^{(1)} &= w^{(0)} - \alpha_m \Delta\tau R^*(w^0) \\ &\cdots \\ w^{(m+1)} &= w^{(0)} - \alpha_m \Delta\tau R^*(w^{(m-1)}) \\ &\cdots \\ w^{n+1} &= w^{(p)} \end{aligned} \tag{9}$$

The additional unsteady source term shifts the Fourier footprint of the spatial discretisation along the negative real axis.[5] In order to prevent instabilities triggered by small real time steps, an approach similar to Melson et al.[6] is taken, such that at each stage of the Runge-Kutta scheme, Δw^n is treated implicitly by setting w^{n+1} equal to $w^{(m+1)}$ and moving it to the left hand side,

$$w^{(m+1)} = w^n - \alpha_m \Delta\tau^* \left(-\frac{\mathcal{V}}{2\Delta t}\Delta w^{n-1} + R(w^{(m)}) \right) \tag{10}$$

where

$$\Delta\tau^* = \frac{\Delta\tau}{\left(1 + \alpha_m \frac{3\mathcal{V}\Delta\tau}{2\Delta t}\right)}$$

which in effect, rescales the pseudo-time step to maintain stability of the Runge-Kutta scheme.

If the inner iterations converge fast enough, the solution to the fully nonlinear BDF is obtained, giving an efficient A-stable scheme which allows very large real time step Δt. However, there is no way of assessing accuracy unless the inner iterations are fully converged. In addition, the scheme becomes very expensive if a large number of inner iterations are required. This motivates the search for alternative schemes which could be less expensive.

Linearized Backward Difference Formula

Another approach to decouple the nonlinear equations of the fully implicit BDF (7) is to linearize $R\left(w_{i,j}^{n+1}\right)$ by

$$R(w^{n+1}) = R(w^n) + \frac{\partial R(w^n)}{\partial w}\Delta w^n + \mathcal{O}\left|\left|\Delta w\right|\right|^2 \tag{11}$$

Given that

$$\frac{\partial R(w^n)}{\partial w} = \frac{\partial}{\partial w}\left(\frac{\partial F_i}{\partial X_i}\right) = \frac{\partial}{\partial X_i}\frac{\partial F_i}{\partial w}$$

and

$$A = \frac{\partial F_1}{\partial w}, \quad B = \frac{\partial F_2}{\partial w}$$

we can then derive the linearized BDF by approximating the flux vectors as

$$\begin{aligned} F_1(w^{n+1}) &= F_1(w^n) + A\Delta w^n + \mathcal{O}\left|\left|\Delta w\right|\right|^2 \\ F_2(w^{n+1}) &= F_2(w^n) + B\Delta w^n + \mathcal{O}\left|\left|\Delta w\right|\right|^2 \end{aligned}$$

where $\Delta w^n = w^{n+1} - w^n$ and A, B are typically known as the flux Jacobians. Linearize equation (7) and multiply everything by $\frac{2\Delta t}{3\mathcal{V}}$

$$\begin{aligned} w_{i,j}^{n+1} - \frac{4}{3}w_{i,j}^n + \frac{1}{3}w_{i,j}^{n-1} + \frac{2\Delta t}{3\mathcal{V}}\left(D_{X_1}A + D_{X_2}B\right)\Delta w_{i,j}^n \\ + \frac{2\Delta t}{3\mathcal{V}}R\left(w_{i,j}^n\right) = \mathcal{O}\left|\left|\Delta w\right|\right|^2 \end{aligned}$$

then rewrite the equation with time differences in delta form to obtain the linearized BDF

$$\begin{aligned} \left\{ I + \frac{2\Delta t}{3\mathcal{V}}\left(D_{X_1}A + D_{X_2}B\right) \right\}\Delta w_{i,j}^n = \\ \frac{1}{3}\Delta w_{i,j}^{n-1} - \frac{2\Delta t}{3\mathcal{V}}R\left(w_{i,j}^n\right) + \mathcal{O}\left|\left|\Delta w\right|\right|^2 \end{aligned} \tag{12}$$

In two space dimensions, this equation can be solved by a single inversion of a large matrix on the left hand side. Due to the fact that $||\Delta w|| = \mathcal{O}(\Delta t)$, the scheme is still second order accurate in time. The cost of the inversion makes this scheme impractical, which leads to the next method.

Alternating Direction Implicit (ADI) Scheme with the Backward Difference Formula (BDF)

In order to reduce the cost of inversion of the linearized BDF, an approximate factorization of the left hand side is introduced. This yields the ADI-BDF scheme.

$$\left[I + \tfrac{2\Delta t}{3\mathcal{V}} D_{X_1} A\right]\left[I + \tfrac{2\Delta t}{3\mathcal{V}} D_{X_2} B\right]\Delta w^n = \frac{1}{3}\Delta w^{n-1} - \frac{2\Delta t}{3\mathcal{V}} R(w^n) \tag{13}$$

This scheme can be solved in 2 steps. First, find the intermediate value $\overline{\Delta w}$ via block tridiagonal inversions

$$\left(I + \frac{2\Delta t}{3\mathcal{V}} D_{X_1} A\right)\overline{\Delta w}^n_{i,j} = \frac{1}{3}\Delta w^{n-1}_{i,j} - \frac{2\Delta t}{3\mathcal{V}} R(w^n_{i,j}) \tag{14}$$

Then, solve for $\Delta w^n_{i,j}$ by yet another block tridiagonal inversion

$$\left(I + \frac{2\Delta t}{3\mathcal{V}} D_{X_2} B\right)\Delta w^n_{i,j} = \overline{\Delta w}^n_{i,j} \tag{15}$$

The ADI scheme is nominally second order accurate in time with three sources of error:

1. discretization error of the BDF,
2. linearization error, and
3. factorization error.

The ADI scheme can be solved at low computational cost with two simple block tridiagonal inversions. However, in practice, the factorization error dominates when Δt is too large, and the scheme is not amenable to parallel processing: it may lose its stability if applied separately in each of a large number of blocks.

Hybrid Scheme

In order to overcome deficiencies within the ADI-BDF scheme and within the dual-time-stepping scheme mentioned earlier, we propose a hybrid scheme designed to combine the advantages of the dual-time-stepping scheme with those of the linearized ADI scheme. This scheme will take an initial ADI step in real time:

$$\left[I + \tfrac{2\Delta t}{3\mathcal{V}} D_{X_1} A\right]\left[I + \tfrac{2\Delta t}{3\mathcal{V}} D_{X_2} B\right]\Delta w^{(1)} + \frac{2\Delta t}{3\mathcal{V}} R(w^n) - \frac{1}{3}\Delta w^{n-1} = 0 \tag{16}$$

yielding a nominal second order accuracy result without iterations. Then, apply the iterative multistage dual-time-stepping scheme augmented by multigrid

$$\Delta w^{(k+1)} - \Delta w^{(k)} + \beta_k\left[\Delta w^{(k)} + \tfrac{2\Delta t}{3\mathcal{V}} R\left(w^{(k)}\right) - \tfrac{1}{3}\Delta w^{n-1}\right] = 0 \tag{17}$$

to drive the solution towards the steady state limit in pseudo-time and recover the fully nonlinear BDF.

The main advantage of this scheme is that the initial ADI step is already formally $\mathcal{O}(\Delta t^2)$, and it can be shown that any subsequent change in the solution due to the additional dual-time-stepping iterations should retain the $O(\Delta t^2)$ accuracy. Subtracting (16) multiplied by β_1 from (17) with $k = 1$ yields the difference in the solution due to the subsequent iteration

$$\begin{aligned}\Delta w^{(2)} - \Delta w^{(1)} &= \beta_1 \frac{4\Delta t^2}{9\mathcal{V}^2} D_{X_1} A D_{X_2} B \Delta w^{(1)} \\ &\quad + \frac{2\Delta t}{3\mathcal{V}}[R(w^{(1)}) - R(w^n) \\ &\quad - \left(D_{X_1} A + D_{X_2} B\right)\Delta w^{(1)}] \\ &\quad + \mathcal{O}\left(||\Delta w||^2\right) \\ &= \mathcal{O}(\Delta t^2)\end{aligned} \tag{18}$$

Although the ADI-BDF is unconditionally stable,[7] in practice, the factorization error restricts the size of time steps for which sufficient stability and accuracy can be attained. The additional dual-time-stepping iterations serve as a method for stablizing factorization errors of the ADI-BDF scheme. Larger real time steps are thus allowed by the ADI-BDF scheme, which is otherwise restrictive due to the factorization error.

Results

The hybrid scheme defined by equations (16) and (17), along with dual-time-stepping scheme and the ADI-BDF scheme have been applied to a two-dimensional pitching airfoil in the flutter regime. The results of these different schemes are then compared with each other along with an experimental data.[8] Labeled AGARD CT-6, this particular test case is a pitching NACA 64A010 airfoil at a Mach number of .796 and Reynolds number of 12.56 million. The mean angle of attack is zero, with pitching amplitude $\pm 1.01^\circ$ and reduced frequency, defined as

$$\frac{\omega Chord}{2q_\infty} = 0.212$$

Implementation

Both implicit and explicit steps in the hybrid scheme presented in this paper are implemented using a conservative cell-centered finite volume scheme. Within the ADI step, the spatial discretisation of the convective fluxes on the explicit side of the equation uses the

blended first and third order numerical dissipation of the JST Scheme with normalized second difference of the pressure acting as shock sensors.[5] On the implicit side, it is sufficient to use first order accurate Jacobians which corresponds to the dominant terms of the JST Scheme. Within the dual-time-stepping scheme, five-level W-cycle multigrid calculations were performed.

In the inviscid test case, as a result of the periodicity of the O-mesh used, a periodic block tridiagonal is generated on the implicit side of the equation. At about twice the cost of inverting non-periodic block tridiagonal matrices, LU decomposition was used to invert the periodic block tridiagonals. The O-mesh is constructed in such a way that the periodic boundary intersects the relatively small cells at the trailing edge of the airfoil. The inclusion of the periodic terms in the block tridiagonal matrix is beneficial.

As for the viscous test case, calculations were performed on a C-mesh for the same airfoil as the inviscid test case. The Baldwin Lomax turbulence model was used for solving the Reynolds-Averaged Navier-Stokes equations. The cross derivative terms in the implicit Jacobians of the ADI-BDF scheme were dropped for simplicity.

Inviscid Results

The inviscid solution is computed on the 160×32 O-mesh shown in figure (1) generated by conformal mapping. Note that the cells at the trailing edge are very small in comparison with those at mid-chord. Hence, with a fixed time step Δt, the CFL number, representing the number of cells traversed by acoustic waves during one time step, is very large near the trailing edge when it is moderate at mid-chord.

Figure (2) shows the resulting lift coefficient versus angle of attack of the three different schemes plotted against experimental results. Both the dual-time-stepping scheme and the hybrid scheme uses 36 real time steps per oscillation period. In each case, 15 multigrid cycles were used per implicit time step; the CFL number is 1764 at the trailing edge and 74 at mid-chord. For the pure ADI calculation, 720 real time steps were required for each oscillation period. The CFL numbers at the trailing edge and mid-chord were 85 and 4 respectively. Instability at the trailing edge prevents the use of a larger time step in the pure ADI case.

Next we show the effect of reducing the number of inner iterations in the hybrid scheme. Figure (3) confirms that the resulting lift coefficient at different angles of attack of the hybrid scheme remains sufficiently accurate with only 4 inner iterations per real time step. This represents a significant reduction of the computational cost; of the order of 60 percent, in comparison with the pure dual-time-stepping scheme.

Comparing the experimental and numerical results in figures (2) and (3), the measurements obtained from the AGARD report consistently demonstrate a slightly smaller total variation of lift, and lie on a slightly broader oval. This may be due to the viscous effects not captured by the Euler Equations.

Viscous Results

The 257×64 C-mesh is shown in figure (4), where only every other grid line is drawn for clarity. The C_L versus α plots of the converged periodic solutions (10^{th} period, 40 inner iterations per real time step) in figure (5) demonstrate that the inclusion of viscous terms have effectively increased the breadth of the oval, producing an approximation closer to the experimental results than those shown by the inviscid calculation.

Figure (6) shows that reducing the number of inner iterations for the hybrid scheme did not change the C_L versus α plots significantly. Ultimately, as few as 4 dual-time-stepping iterations following initial ADI-BDF step are needed for sufficient accuracy. Figure (8) exhibits the plots of C_p distributions of the hybrid scheme with different number of dual-time-stepping iterations corresponding to figure (6). Note that after 10 iterations, all the oscillations in the C_p distributions are greatly reduced.

Figure (9) shows that when only one ADI-BDF step and one dual-time-stepping iteration is applied, the resulting contours of the coefficient of pressure on the upper surface of the airfoil is much closer to the fully converged solution than the two steps of dual-time-stepping iterations.

Figure (7) show the C_p plot of viscous calculations with different time step sizes Δt. The number of real time steps performed to complete one oscillation of the pitching airfoil, $PSTEP$, is varied to demonstrate the second order temporal accuracy of the scheme.

Figures (10) through (13) compares the C_p distribution on the surface of the airfoil at several different phase angles of the converged solutions (i.e., the 10^{th} period of oscillation) for both the viscous and inviscid calculations. Using the hybrid scheme presented, 15 subiterations were performed for the inviscid test case and 30 subiterations for the viscous case. The "+" and "$\times$" symbols represent C_p distribution on the upper and lower surfaces of the airfoil for the viscous calculation. The solid and dashed line represent C_p distribution on the upper and lower surfaces of the airfoil for the inviscid calculation. Due to the unsteadiness of the flow, the nonzero lift at zero pitch angle illustrates the phase lag between the lift and the angle of attack α.

Conclusion

Using a single ADI-BDF step followed by small numbers of iterations driving the solution towards the fully nonlinear BDF, our conclusion shows that we can obtain second order accuracy without the need to iterate to convergence at each real time step. (of the order

of 4 or 5). As a result, the hybrid scheme permits a substantial reduction in the cost for unsteady flow simulations. (i.e., turbomachinery simulation.)

Acknowledgments

This work was funded by the Department of Energy as a part of the ASCI program under contract number LLNL-B341491.

References

[1]Caughey, D. and Jameson, A., "Fast Preconditioned Multigrid Solution of the Euler and Navier-Stokes Equations for Steady Compressible Flows," AIAA Paper 2002–0963, Jan. 2002, AIAA 40th Aerospace Sciences Meeting and Exhibit January 14–17, 2002, Reno, Nevada.

[2]Jameson, A. and Caughey, D., "How Many Steps are Required to Solve the Euler Equations of Steady, Compressible Flow: In Search of a Fast Solution Algorithm," AIAA Paper 2001–2673, Jan. 2001, AIAA 15th Computational Fluid Dynamics Conference June 11–14, 2001, Anaheim, California.

[3]Yoon, S. and Jameson, A., "Lower-Upper Symmetric-Gauss-Seidel Method for the Navier-Stokes equations," *AIAA Journal*, Vol. 26, No. 9, Sept. 1988, pp. 1025–1026.

[4]McMullen, M., Jameson, A., and Alonso, J., "Acceleration of Convergence to a Periodic Steady State in Turbomachinery Flows," AIAA Paper 2001–0152, Jan. 2001, AIAA 39th Aerospace Sciences Meeting, January 8–11,Reno, Nevada.

[5]Jameson, A., "Time Dependent Calculations Using Multigrid, with Applications to Unsteady Flows Past Airfoils and Wings," AIAA Paper 91–1596, June 1991, AIAA 10th Computational Fluid Dynamics Conference, Honolulu HI, June 1991.

[6]N. D. Melson, M. D. S. and Atkins, H. L., "Time-Accurate Navier-Stokes Calculations with Multigrid Acceleration," *Proceedings of the Sixth Copper Mountain Conference on Multigrid Methods*, NASA Conf. Publication–3224, 1993, Copper Mountain, CO.

[7]Beam, R. M. and Warming, R. F., "An Implicit Factored Scheme for the Compressible Navier-Stokes Equations," *AIAA Journal*, Vol. 16, No. 4, 1978, pp. 393–402.

[8]Davis, S., "NACA 64A010 (NASA AMES Model) Oscillatory Pitching," AGARD Compendium of Unsteady Aerodynamic Measurements AGARD–R–702, 1982.

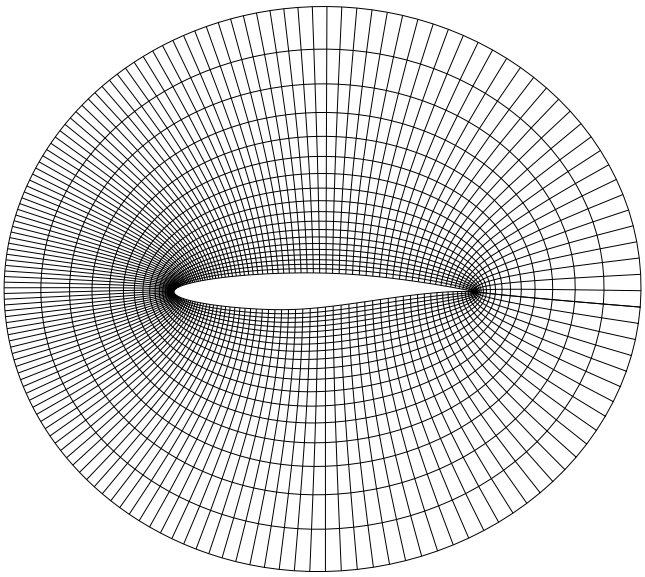

Fig. 1 Inner part of the 160 × 32 O-mesh for the NACA64A010 grid for inviscid calculation

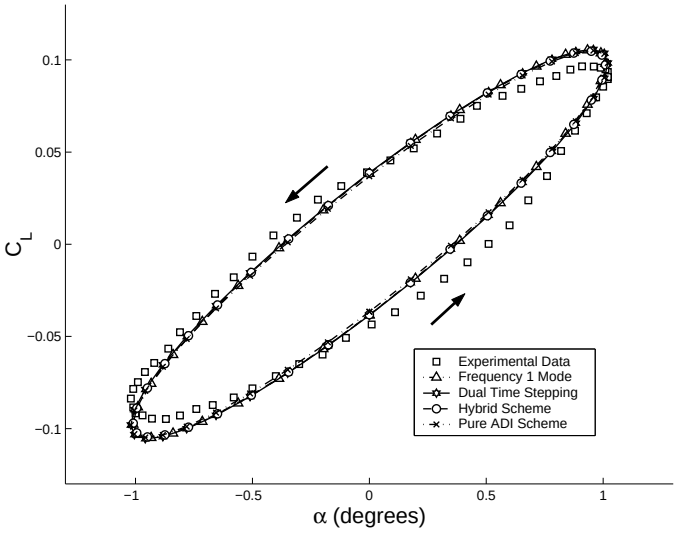

Fig. 2 Comparison of C_L versus α of Different Numerical Schemes for the Inviscid Case

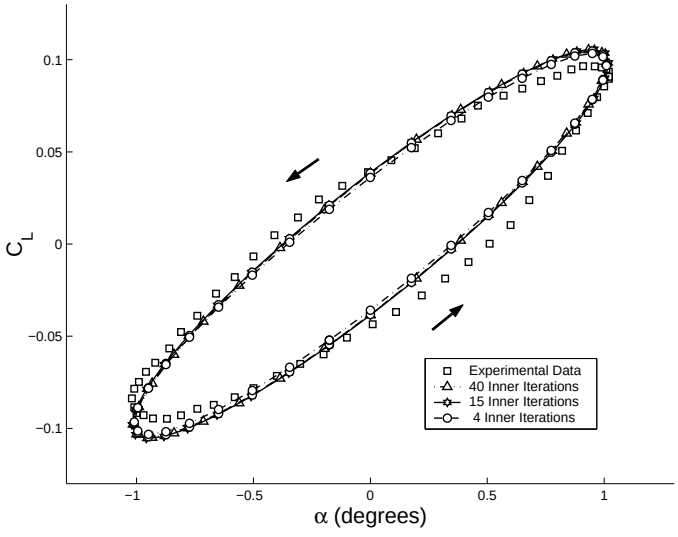

Fig. 3 Comparison of C_L versus α of the Hybrid Scheme with Different Number of Inner Iterations for the Inviscid Case

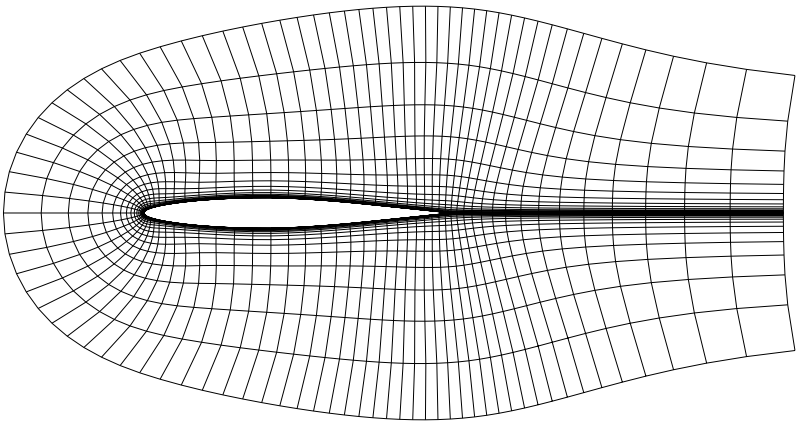

Fig. 4 Inner Part of the 257 × 64 C-mesh for the NACA64A010 grid for Viscous Calculation, every other grid line shown

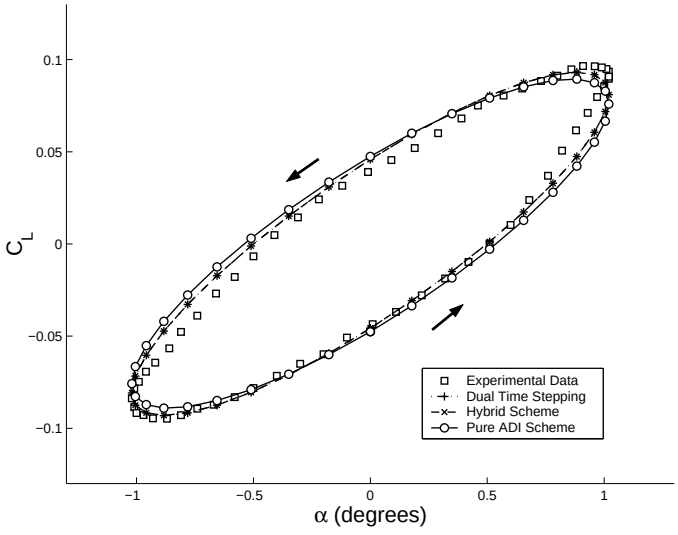

Fig. 5 Comparison of C_L versus α of Different Numerical Schemes for the Viscous Case

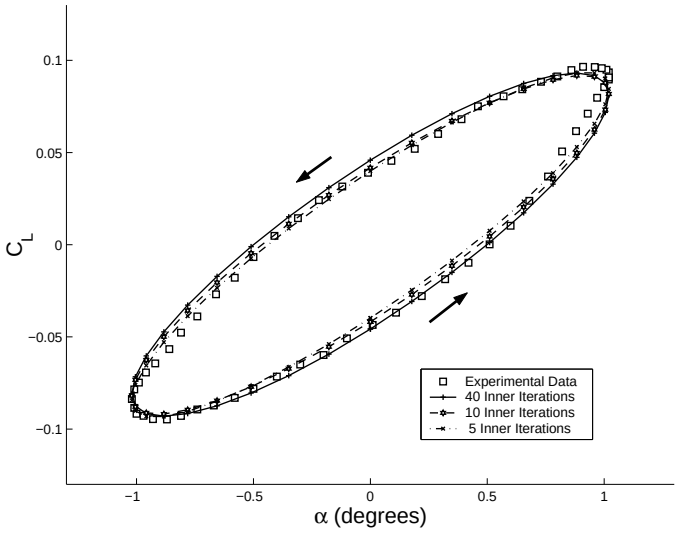

Fig. 6 Comparison of C_L versus α of the Hybrid Scheme with Different Number of Inner Iterations for the Viscous Case

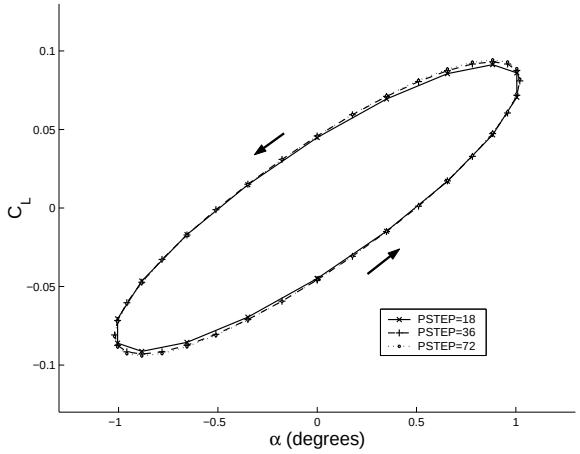

Fig. 7 Demonstration of Temporal Accuracy for the Viscous Case

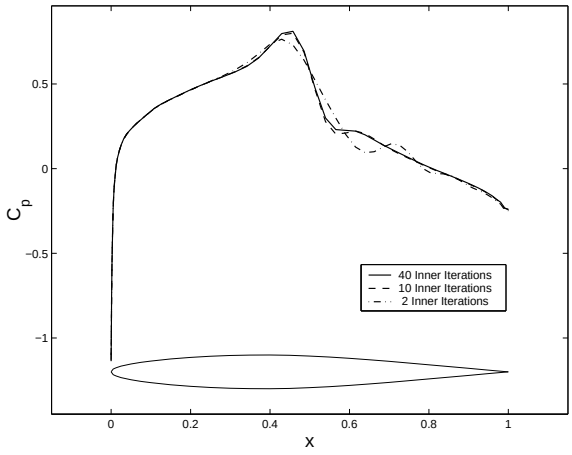

Fig. 8 Pressure Distribution on the NACA64A010 Airfoil at $T = 576$, $\alpha = 0.0^\circ$ and $M = 0.796$ for the Viscous Calculation with the Hybrid Scheme

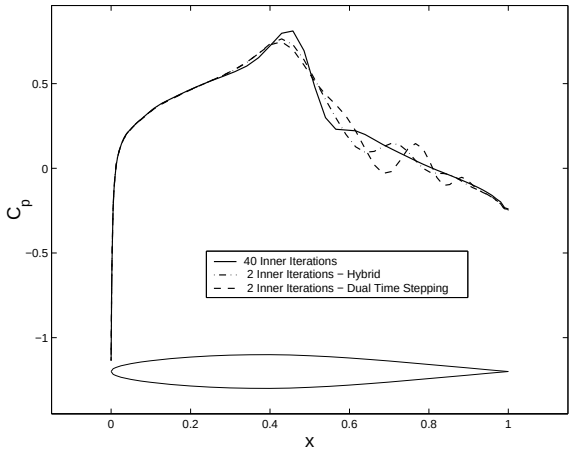

Fig. 9 Pressure Distribution on the NACA64A010 Airfoil at $T = 576$, $\alpha = 0.0^\circ$ and $M = 0.796$ for the Viscous Calculation

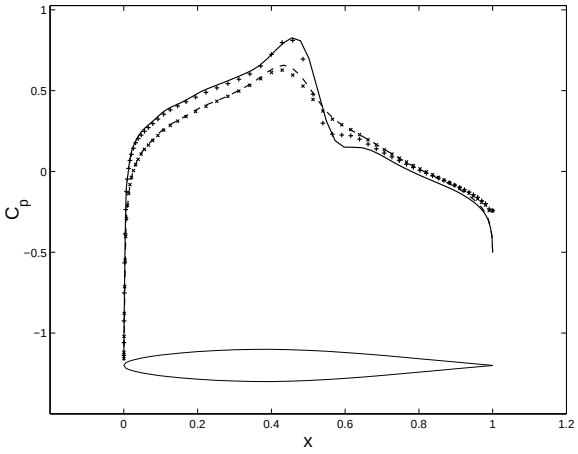

Fig. 10 Pressure Distribution on the NACA64A010 Airfoil at $T = 576$, $\alpha = 0.0^\circ$ and $M = 0.796$

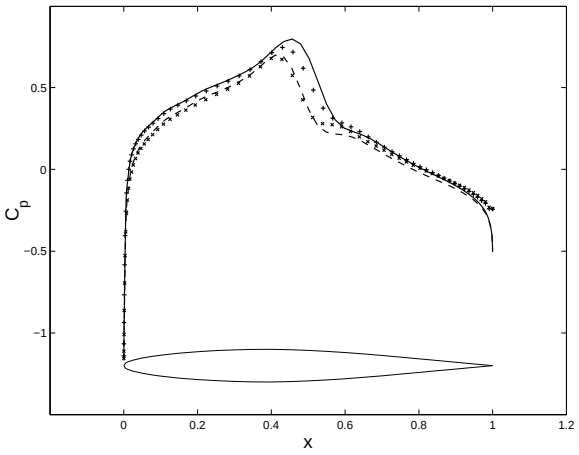

Fig. 11 Pressure Distribution on the NACA64A010 Airfoil at $T = 619$, $\alpha = -0.883^\circ$ and $M = 0.796$

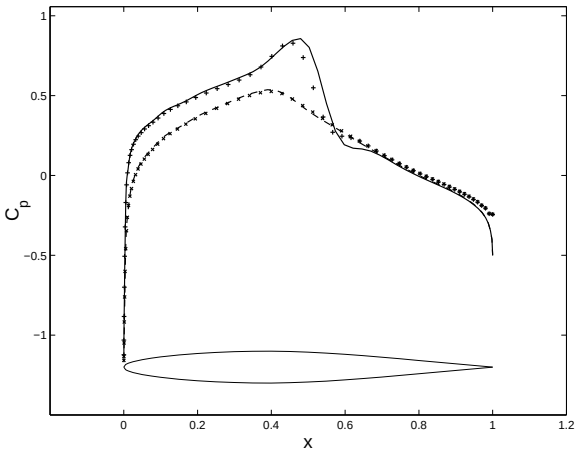

Fig. 12 Pressure Distribution on the NACA64A010 Airfoil at $T = 630$, $\alpha = -0.883^\circ$ and $M = 0.796$

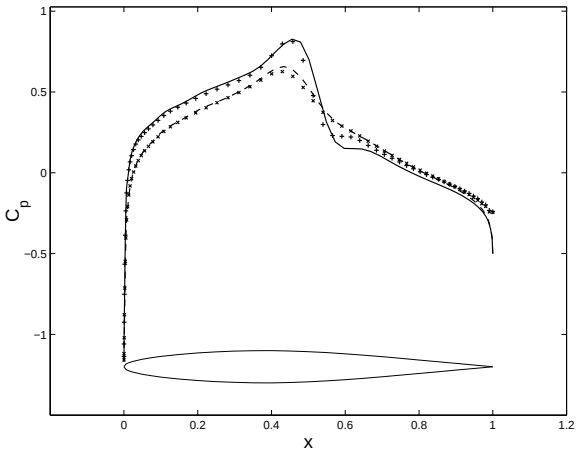

Fig. 13 Pressure Distribution on the NACA64A010 Airfoil at $T = 640$, $\alpha = 0.0^\circ$ and $M = 0.796$